Supplemental material for "Effect of structural relaxation on the electronic structure of graphene on hexagonal boron nitride"

G.J. Slotman,[1] M.M. van Wijk,[1] Pei-Liang Zhao,[2] A. Fasolino,[1] M.I. Katsnelson,[1] and Shengjun Yuan[1,*]

[1] *Institute for Molecules and Materials, Radboud University, Heyendaalseweg 135, 6525AJ Nijmegen, The Netherlands*

[2] *Department of Applied Physics, Zernike Institute for Advanced Materials, University of Groningen, Nijenborgh 4, NL-9747AG Groningen, The Netherlands*

(Dated: September 4, 2015)

RELAXATION AND INFLUENCE OF THE INTERACTION STRENGTH

As the ratio between the lattice constants of graphene and hBN is approximately 55/56, a common supercell can be constructed by repeating 56 × 56 unit cells of graphene on 55 × 55 unit cells of hBN, resulting in a 1.8 % mismatch in lattice constant. We relax only the graphene layer. We assume that a hBN substrate in optimal stacking does not deform and we thus keep the hBN layer fixed to mimic a bulk substrate. Furthermore, in the cases of misaligned graphene on graphite, a comparison of a mobile layer on a rigid substrate to a fully mobile double layer graphene has shown that although the deformations are shared between the two layers in the bilayer, the pattern itself does not change [S1]. To create a common supercell for graphene on hBN under an angle, we rotate the hBN by

$$\theta = \tfrac{1}{2}\arccos\left(\frac{2n^2+2nm-m^2}{2(n^2+nm+m^2)}\right), \tag{S1}$$

resulting in a cell of length

$$a_{cell} = a_{hBN}\sqrt{n^2+nm+m^2}. \tag{S2}$$

where a_{hBN} is the lattice constant of hBN n, m are positive integers with $n > m$.

The graphene layer is not rotated but the unit cell is repeated q times, resulting in a side of length

$$a_{cell} = a_C q, \tag{S3}$$

where q is an integer and the lattice constant of graphene a_C is slightly adjusted to make both supercells the same size. By choosing n,m and q appropriately, stretching is kept to a minimum (<0.01%). From the size of the moiré pattern observed experimentally [S2] one can induce that the lattice constant of graphene is very close to the equilibrium value, meaning that there is minimal stretching. The effect of stretching globally is shown in Ref. [S3] for an extreme case of stretching 0.9 % and the effect is quantitative, enhancing the adjustment to the substrate. For the REBO [S4] potential as implemented in LAMMPS [S5] the equilibrium bond length of graphene is 1.3978 Å. We thus set a_C to this value and scale a_{hBN} accordingly. After relaxation, we rescale a_C in the relaxed structure to 1.42 Å prior to the TB calculations. The length λ of the moiré wavelength is given by [S6]:

$$\lambda = \frac{p}{\sqrt{1+p^2-2p\cos(\theta)}}a, \tag{S4}$$

where p is a_C/a_{BN}.

The interaction strength between the substrate and graphene can be tuned. We introduce a scaling factor s as the ratio of the C-B interaction with respect to the C-N interaction and indicate with r the C-N interaction multiplication factor compared to the original C-C interaction of the Kolmogorov-Crespi potential [S7]. Throughout the paper, we have used $s = 30$ % and $r = 2$, meaning that the C-B interaction is 60 % of the original C-C value and the C-N interaction 200 % of the original value, as these values match well with both experimental results [S2] and *ab initio* total energy calculations [S8, S9]. Since there are not yet sufficient data available for more precise benchmarking, we show the effect of changes in these parameters.

Figure S1 and S2 show the influence of this scaling on the bond length and on-site potential, respectively. For higher interaction strengths the effect of the relaxation increases, causing bigger changes in the tight-binding parameters. From left to right there is an inversion from negative on-site potentials in the centre of the hexagons to positive values. This corresponds to the transition in bond length shown in [S3]. A similar dependence can be found in the density of states (DOS), as seen in figure S3. The DOS is more distorted with increasing interactions strength r. Decreasing s causes the peak to shift from the electron side to the hole side.

COMPARISON OF DIFFERENT TB MODELS

In figure S4 we show the moiré patterns after structural relaxation for different rotation angles θ, and compare the on-site potentials calculated by using our TB model and the one proposed by Ref. [S10], which is based on an effective TB Hamiltonian in [S11]. As one can see from the different length scales used in different moiré patterns, the increase of θ leads to smaller changes of the atomic (bond) distance, which is consistent with the experimental observations. As a consequence, in our TB model, the change of the TB parameters (hopping terms and on-site potentials) is more

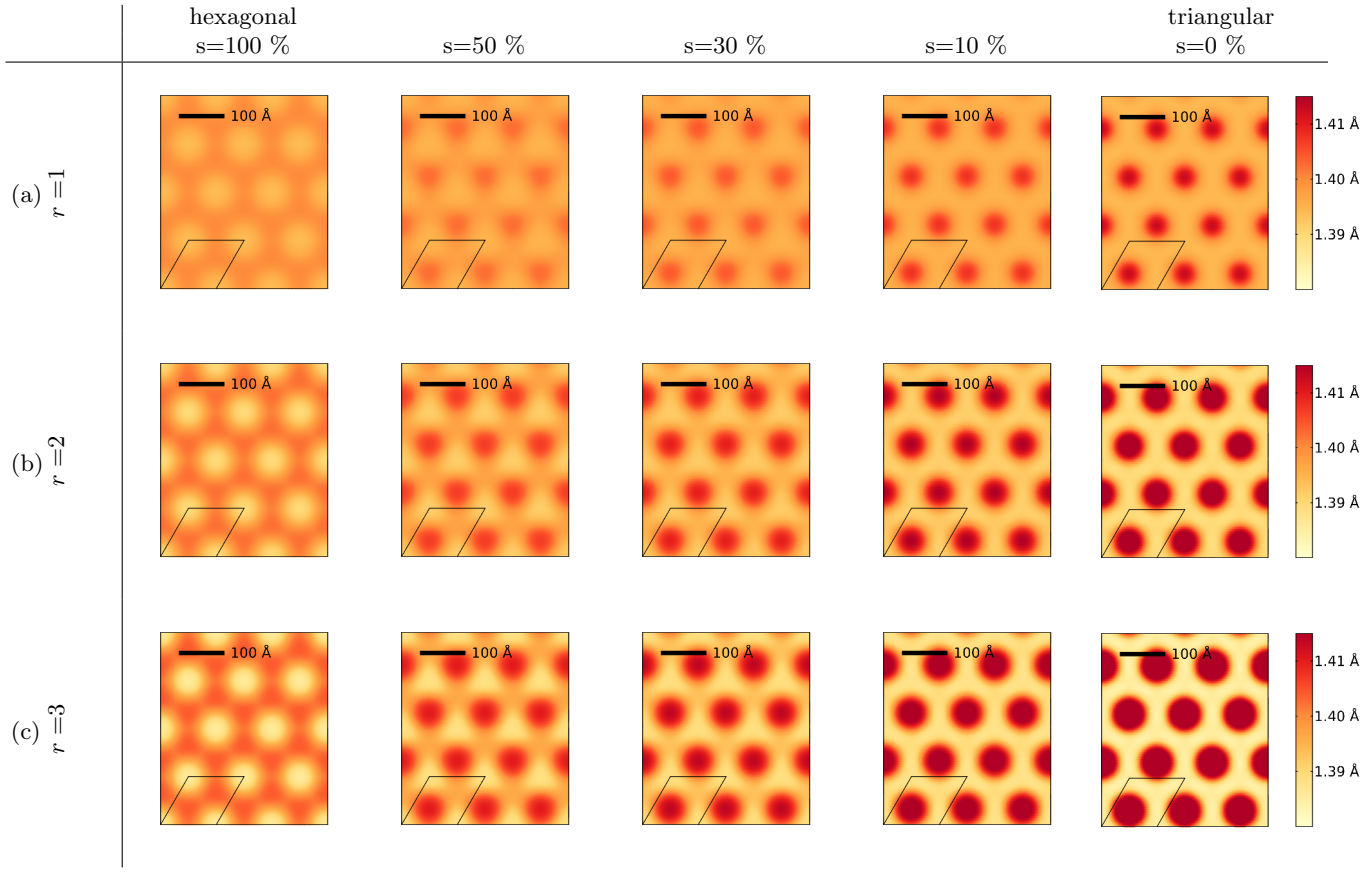

FIG. S1. The bond length as function of the scaling between the C-B and C-N interaction. For $s = 100\%$ both interactions are the same, while for $s = 0\%$ only the C-N interaction is taken into account. The total interaction strength is increased from top to bottom. The equilibrium bond length is 1.3978 Å.

significant with smaller θ. If the local gap term is included, it is possible to keep the change of the on-site potentials in the same level for different θ. However, since the local gap term does not renormalize the hopping energies, the amplitude of the extra Dirac points in the DOS is reduced with larger θ, as shown in figure S5, where we compare the DOS calculated by using our TB model and the one proposed in Ref. [S10]. The TB model proposed in Ref. [S10] is valid only for small rotation angles, and the corresponding results are in good agreements with ours if the local gap term $\Delta U = 32$ meV is included in our model. However we want to emphasise that the microscopic origin of the TB models are different as there is no structure relaxation in Ref. [S10].

There are experimental evidences that the extra Dirac points disappear for large θ. For example, Ref. [S12] shows that graphene-hBN structures with moiré length $\lambda = 3.8$ nm and $\lambda = 3.5$ nm do not have additional peaks in the resistivity, and Refs. [S13, S14] give $\theta < 1^\circ$ as an upper bound for the observation of these superlattice effects. This feature is captured also in our TB model, with local gap term $\Delta U = 32$ meV or larger.

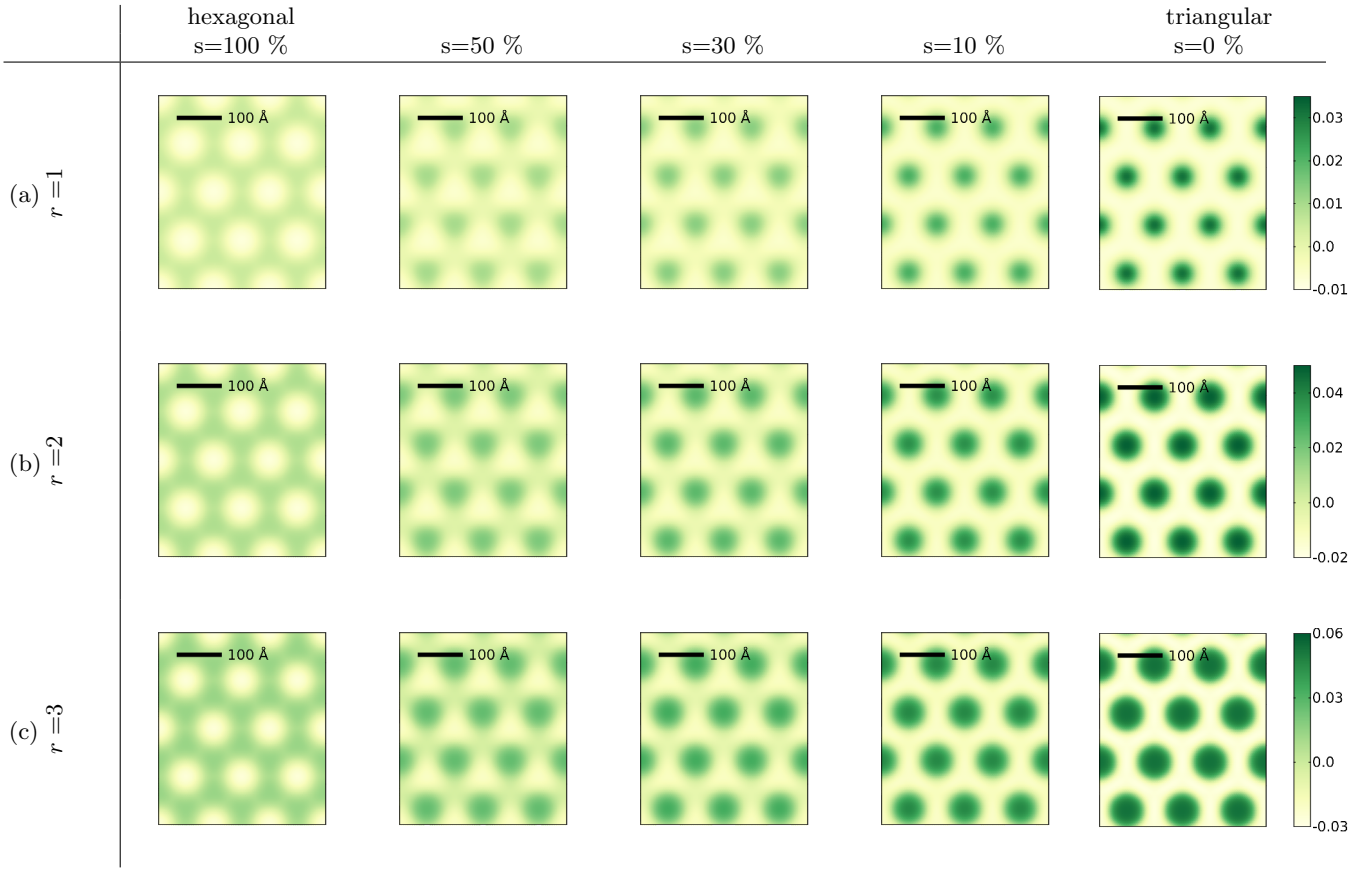

FIG. S2. The on-site potential as function of the scaling between the C-B and C-N interaction. For $s = 100\%$ both interactions are the same, while for $s = 0\%$ only the C-N interaction is taken into account. The total interaction strength is increased from top to bottom.

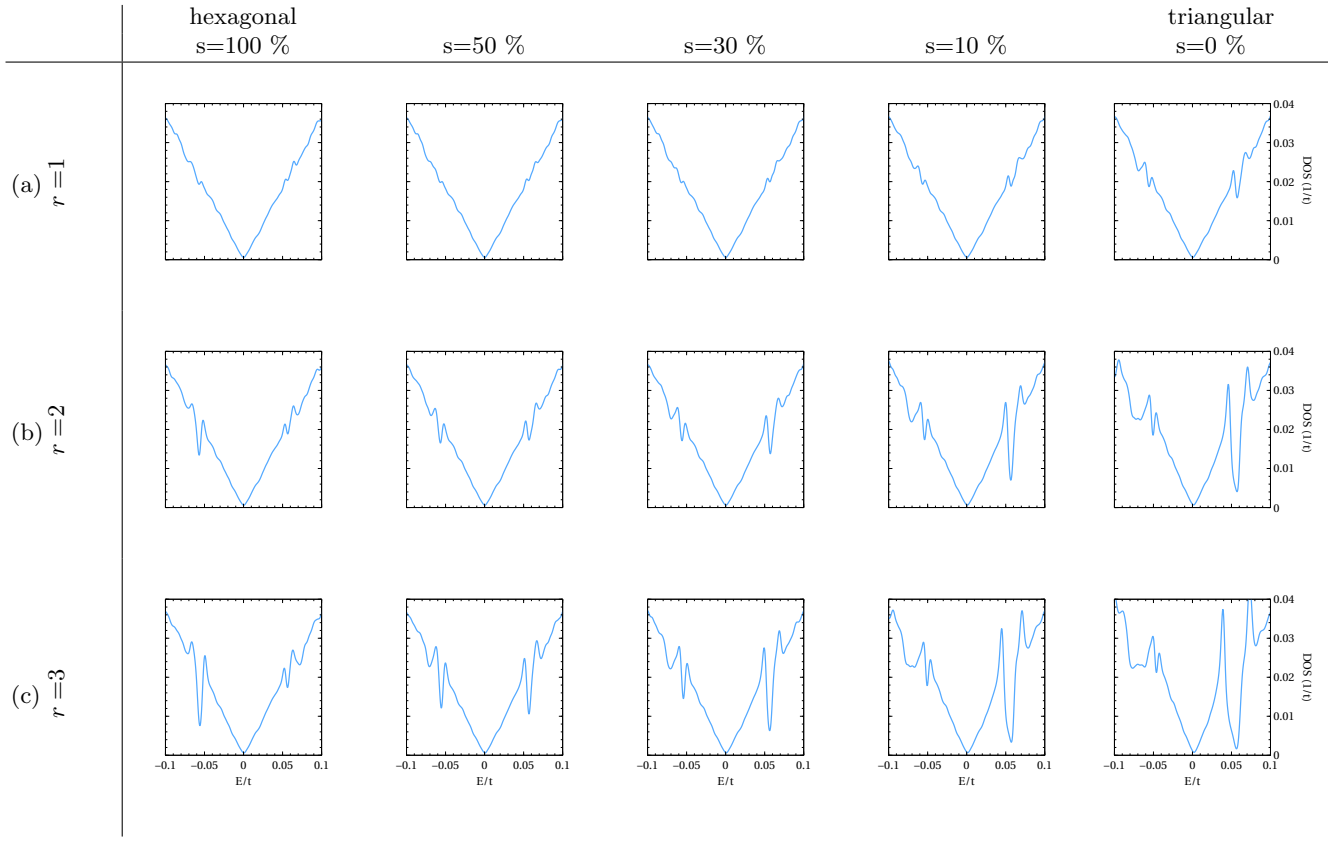

FIG. S3. The DOS as a function of the scaling between the C-B and C-N interaction. For $s = 100\%$ both interactions are the same, while for $s = 0\%$ only the C-N interaction is taken into account. The total interaction strength is increased from top to bottom.

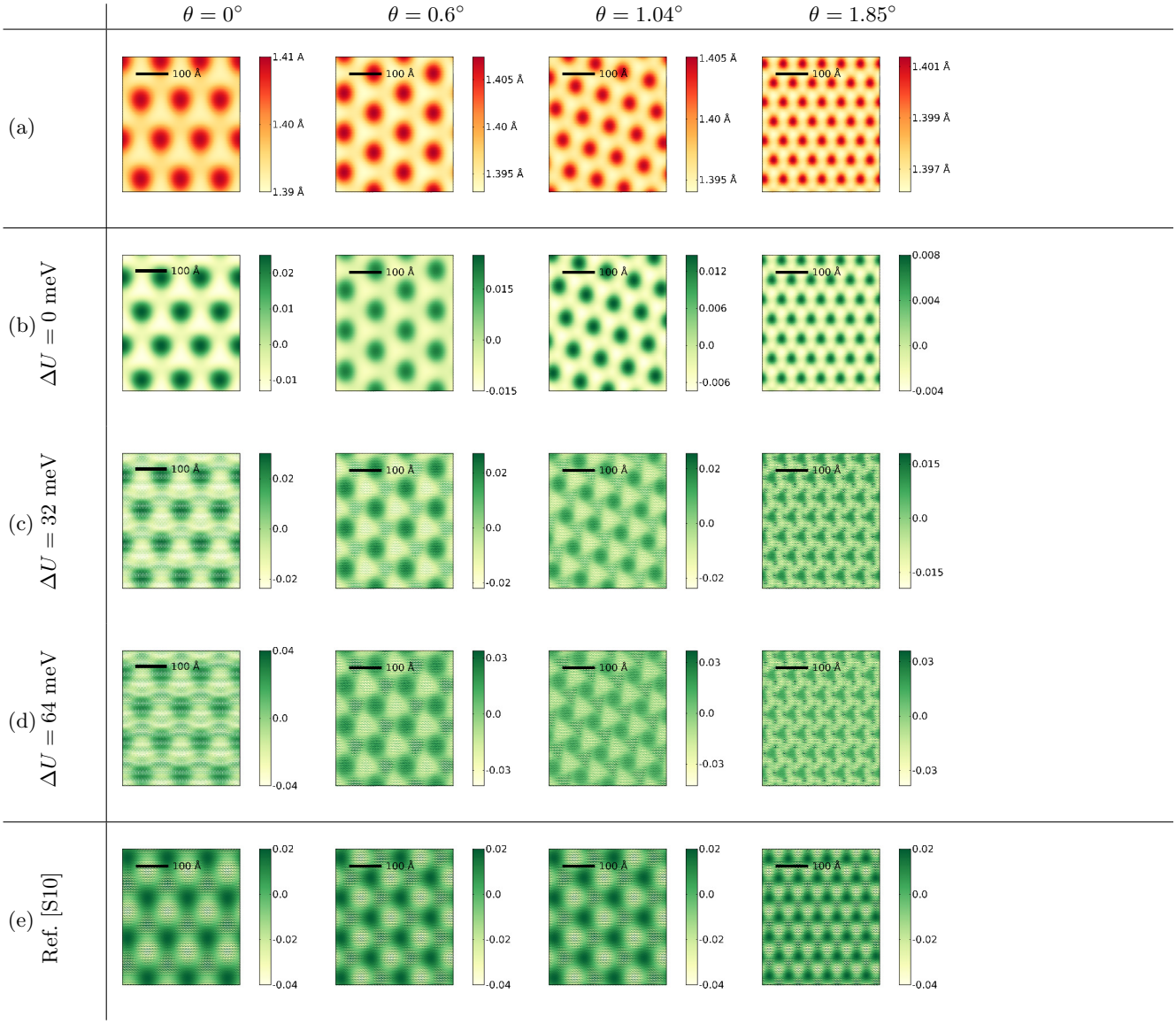

FIG. S4. For different rotation angles θ the figure shows (a) the bond length after relaxation, (b)-(d) the on-site potential for different ΔU in our TB model and (e) the on-site potential for the superlattice Hamiltonian given by Diez *et al.* [S10].

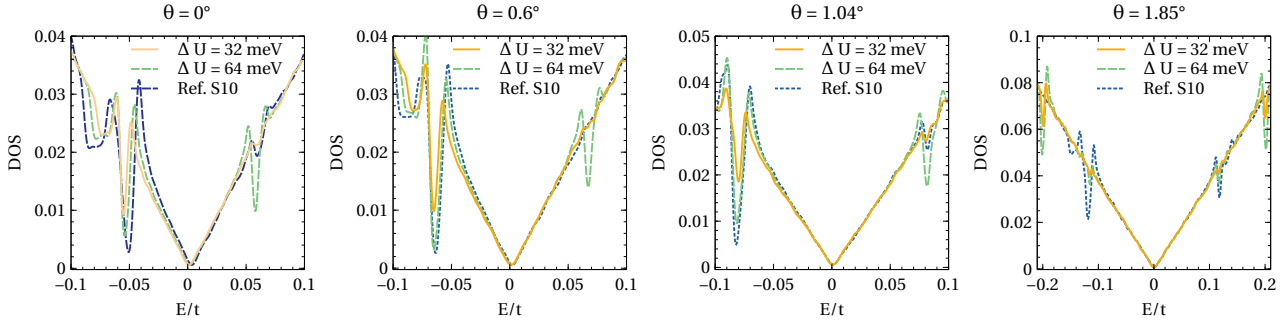

FIG. S5. The DOS for $\Delta U = 32$ meV, $\Delta U = 64$ meV and for the superlattice tight-binding Hamiltonian given by Ref. [S10]. The rotation angle θ increases from left to right.

* s.yuan@science.ru.nl

[S1] M. M. van Wijk, A. Schuring, M. I. Katsnelson, and A. Fasolino, 2D Materials **2**, 034010 (2015).
[S2] C. R. Woods, L. Britnell, A. Eckmann, R. S. Ma, J. C. Lu, H. M. Guo, X. Lin, G. L. Yu, Y. Cao, R. V. Gorbachev, A. V. Kretinin, J. Park, L. A. Ponomarenko, M. I. Katsnelson, Y. N. Gornostyrev, K. Watanabe, T. Taniguchi, C. Casiraghi, H.-J. Gao, A. K. Geim, and K. S. Novoselov, Nat. Phys. **10**, 451 (2014).
[S3] M. M. van Wijk, A. Schuring, M. I. Katsnelson, and A. Fasolino, Phys. Rev. Lett. **113**, 135504 (2014).
[S4] D. W. Brenner, O. A. Shenderova, J. A. Harrison, S. J. Stuart, B. Ni, and S. B. Sinnott, J. Phys.: Condensed Matter **14**, 783 (2002).
[S5] S. Plimpton, J. Comput. Phys. **117**, 1 (1995).
[S6] K. Hermann, J. Phys. Condensed Matter **24**, 314210 (2012).
[S7] A. N. Kolmogorov and V. H. Crespi, Phys. Rev. B **71**, 235415 (2005).
[S8] B. Sachs, T. O. Wehling, M. I. Katsnelson, and A. I. Lichtenstein, Phys. Rev. B. **84**, 195414 (2011).
[S9] M. Bokdam, T. Amlaki, G. Brocks, and P. J. Kelly, Phys. Rev. B **89**, 201404 (2014).
[S10] M. Diez, J. P. Dahlhaus, M. Wimmer, and C. W. J. Beenakker, Phys. Rev. Lett. **112**, 196602 (2014).
[S11] J. R. Wallbank, A. A. Patel, M. Mucha-Kruczyński, A. K. Geim, and V. I. Fal'ko, Phys. Rev. B **87**, 245408 (2013).
[S12] B. Hunt, J. D. Sanchez-Yamagishi, A. F. Young, M. Yankowitz, B. J. LeRoy, K. Watanabe, T. Taniguchi, P. Moon, M. Koshino, P. Jarillo-Herrero, and R. C. Ashoori, Science **340**, 1427 (2013).
[S13] L. A. Ponomarenko, R. V. Gorbachev, G. L. Yu, D. C. Elias, R. Jalil, A. A. Patel, A. Mishchenko, A. S. Mayorov, C. R. Woods, J. R. Wallbank, M. Mucha-Kruczynksi, B. A. Piot, M. Potemski, I. V. Grigorieva, K. S. Novoselov, F. Guinea, V. I. Fal'ko, and A. K. Geim, Nature **497**, 594 (2013).
[S14] M. Yankowitz, J. Xue, D. Cormode, J. D. Sanchez-Yamagishi, K. Watanabe, T. Taniguchi, P. Jarillo-Herrero, P. Jacquod, and B. J. LeRoy, Nature Physics **8**, 382 (2012).